The following publication D. Weng, M. Cai, W. Chen, J. Wang and S. Ji, "GNSS Fault Detection and Exclusion (FDE) Under Sidewalk Constraints for Pedestrian Localization in Urban Canyons," in IEEE Transactions on Intelligent Transportation Systems, vol. 25, no. 9, pp. 11168-11179, Sept. 2024 is available at https://doi.org/10.1109/TITS.2024.3361069.

GNSS Fault Detection and Exclusion (FDE) under Sidewalk Constraints for Pedestrian Localization in Urban Canyons

Duojie Weng, Miaomiao Cai, Wu Chen, Jingxian Wang, Shengyue Ji

***Abstract*—The Global Navigation Satellite System (GNSS) has gained widespread use in smartphones, providing support for various pedestrian applications. In urban areas, multipath effects introduce large errors in different measurements, severely degrading the GNSS accuracy. To mitigate multipath effects, several Fault Detection and Exclusion (FDE) methods have been developed. However, in urban canyons, their effectiveness is significantly degraded due to the lack of fault-free measurements in the cross-street direction. In urban canyons, the pedestrian network provides an opportunity to improve the urban GNSS accuracy for pedestrians. The purpose of this study is to improve the GNSS FDE performance through the sidewalk constraints. A new scheme has been proposed to distinguish the correct side of the street effectively. The Hough Transform estimator was used to find the most consistent GNSS measurements under sidewalk constraints. To assess the proposed algorithm's performance, extensive tests were conducted in urban canyons. The analysis of Carrier-to-Noise density ratio (C/N0) shows that 92% of sidewalks can be distinguished from the opposite sidewalk along the same street. The static test shows that the positioning accuracy can be improved from 22 m to 4.9 m, a 77% improvement over the residual based FDE. The dynamic test showed that the proposed method can achieve the sidewalk positioning, which is essential for many pedestrian applications such as last-mile delivery, emergency caller positioning and jaywalking monitoring.**

***Index Terms*—GNSS, Pedestrian map, smartphone, urban canyons**

I. Introduction

Global Navigation Satellite System (GNSS) receivers have become ubiquitous in smartphones, benefiting numerous location-based applications in our everyday lives [1-3]. While most of GNSS errors can be reduced by using Differential GNSS (DGNSS) or the advanced modelling techniques [4, 5], multipath effects pose a unique challenge. Unlike other errors, multipath effects are closely related to the local environment of the receiver and cannot be addressed by using DGNSS or modelling techniques. Consequently, mitigation of multipath effects has become a long-standing challenge for GNSS communities.

This work is supported by Hong Kong General Research Fund (15230823) and the Open fund of State Key Laboratory of Satellite Navigation System and Equipment Technology (CEPNT2022A02). (Corresponding author: *Wu Chen*)

Duojie Weng and Wu Chen are with the Department of Land Surveying and Geo-Informatics, The Hong Kong Polytechnic University, Hong Kong (e-mail: wengduojie.lsgi@polyu.edu.hk; wu.chen@polyu.edu.hk;).

Miaomiao Cai and Jingxian Wang are with the Department of Land Surveying and Geo-Informatics, The Hong Kong Polytechnic University, Hong Kong (e-mail: mmcai@outlook.com; jingxian.wang@ connect.polyu.hk;).

Shengyue Ji is with the College of Oceanography and Space Informatics, China University of Petroleum (East China), Qingdao 266580, China (e-mail: 19990045@upc.edu.cn).

Multipath effects are caused by two different phenomena: multipath reception and non-line-of-sight (NLOS) receptions. Multipath reception refers to a phenomenon that the direct line-of-sight (LOS) and the reflected signals are received simultaneously, while NLOS reception represents that the direct GNSS signal is blocked, and signals are received only through the reflected paths [6-8]. These signals cause measurement errors up to tens or even hundreds of meters [9]. Failure to cope with these signals results in a positioning error as large as tens of meters, especially in the cross-street direction [10-12]. Therefore, in urban areas, the current GNSS technique could not meet meter level accuracy, which is urgently needed by many applications including COVID-19 tracking, ride-sharing services, location-based augmented reality, last-mile delivery, social networking, and emergency caller positioning [8, 13].

Extensive studies have been carried out to mitigate multipath effects [11, 12, 14, 15]. For commercially available GNSS receivers, multipath effects can be mitigated using two distinct methods: (1) estimation of multipath errors, and (2) detection and elimination of faulty measurements resulting from multipath effects. The former approach uses advanced estimation algorithms such as particle filtering [2], factor graph optimization [16], and sparse estimation [17] to determine the estimates of multipath errors. In this study, however, our focus will primarily be on the latter methods, which involve the detection and elimination of faulty measurements influenced by multipath effects.

The initial attempts to detect and exclude faulty GNSS measurements were pioneered by the Receiver Autonomous Integrity Monitoring (RAIM) methods, which were developed mainly for aviation application in the 1980s [14, 18]. Due to their simplicity, self-sufficiency, and effectiveness, these RAIM methods have been widely used in aircraft receivers [19]. During that time, most of them were designed for the single fault, where the probability of multiple faults can almost be neglected [19]. However, for civilian users in urban areas, these RAIM algorithms fail to detect and exclude multiple GNSS faults that occur frequently due to signal blockages and reflections [11, 19, 20].

A variety of Fault Detection and Exclusion (FDE) algorithms have been proposed to tackle the challenges of multiple GNSS faults in urban environments. These algorithms can be broadly classified into three categories: quality control method, residual based FDE, and solution separation based FDE. The quality control method, as the first category, detects multipath and NLOS signals by analyzing various features such as elevation angle, carrier-to-noise density ratio (C/N0), and azimuth angle

[21-23]. These features are compared against predefined thresholds to identify multipath or NLOS signals. However, this method could not identify them reliably due to significant overlaps between normal measurements and faulty measurements. Since NLOS or multipath signals could not be reliably identified using only one feature, various intelligent algorithms have been developed to enhance the identification performance by incorporating these features [24, 25].

The second type of methods involves the enhancement of conventional RAIM algorithms to cope with multiple faults [11]. They employ a residual based FDE algorithm that iteratively excludes measurements with the largest residuals until the test statistic falls within the threshold. However, when a large portion of faulty measurements are observed by receivers in urban canyons, the largest residual does not necessarily mean the corresponding measurement has a fault. Under this condition, the residual based FDE frequently eliminates fault-free measurements while keeping some faulty measurements, resulting in a large positioning error [26].

The third type of FDE methods is based on the bottom-up search method, also known as solution separation method. This approach involves exhaustively evaluating all subsets of satellites and considering the most consistent measurements as fault-free ones [27-30]. In urban canyons, however, the cross-street redundancy is severely reduced, and the performance of these methods is significantly degraded [31]. Moreover, evaluating all subsets of measurements exhaustively can impose a heavy computational burden, especially when there are tens of measurements from the receiver [32]. To address this issue and reduce the computational cost, random sample of consensus (RANSAC) algorithm has been applied in GNSS to find the most consistent measurements[33, 34].

In recent years, the rapid development of GNSS and the high-sensitivity receiver technique have greatly increased the number of visible satellites on a smartphone. In relatively open areas, the large number of GNSS measurements benefit the accurate and reliable position solutions, improving the positioning coverage. In urban canyons with dense buildings, however, the majority of GNSS measurements are affected by multipath or NLOS errors, and often there are not sufficient fault-free satellites received from the cross-street direction[26, 35]. This geometry problem has become a challenge for current FDE algorithms, degrading the GNSS accuracy in urban areas [26, 35, 36].

In recent years, external data have been extensively explored to the GNSS accuracy in urban canyons [31]. One approach is GNSS solution under constraints of height, which can be derived from maps or pressure sensors [12, 37]. This method reduces the number of unknowns from 4 to 3 and improves the horizontal Dilution of precision (DOP) values. Therefore, the horizontal positioning accuracy can be improved through the height constraints. Another method is to detect and exclude the NLOS satellites that are obtained from nearby sensor-rich vehicles [38, 39]. This method assumes that the similar LOS/NLOS signals are shared around a building. However, the multipath and NLOS errors change significantly even when the user moves little in the cross-street direction. Furthermore, 3D building models have been treated as a complementary data source for urban GNSS positioning since most of GNSS multipath and NLOS signals are attributed to buildings [8, 35, 40-42]. One of the popular techniques is the shadow matching method, which determines positions based on the fact that different LOS signals can be observed at different locations due to the blockage of buildings [35, 41]. It has laid a theoretical foundation for improving the positioning accuracy of mobile phones, particularly in cross-street directions. However, the performance of this method in the along-street direction is limited, especially when buildings along the street have similar heights [43-45]. Furthermore, the availability of accurate 3D models can be a challenge in some cities.

The use of road maps has significantly improved the positioning performance of vehicles [15, 46-48]. In urban canyons with tall buildings, pedestrians should stay in footpaths on both sides of the street to keep themselves safe. Pedestrian maps provide a comprehensive network of pedestrian pathways, including sidewalks, crosswalks, and underpasses, represented by their centerlines. The line segments or polylines in these maps can be used as constraints for pedestrian positioning. However, few studies have been carried out to solve GNSS positions under sidewalk constraints. Notably, pedestrian networks are publicly available in various cities such as Hong Kong and Seattle. Moreover, they are extensively used in popular mapping platforms like Google Maps and OS Maps to facilitate pedestrian navigation. In cases where pedestrian network data are is unavailable, it is still possible to gather information about the entire sidewalk by determining the coordinates of specific control points along the pathway. This approach is particularly suitable when sidewalks can be represented as line segments.

The objective of this study is to enhance the performance of GNSS FDE by incorporating cross-street constraints. We will first demonstrate that the use of the residual based FDE under the sidewalk constraints can lead to frequent incorrect identification of sidewalks, especially in urban areas with dense pedestrian networks. Therefore, new methods are necessary to mitigate the impact of unqualified sidewalks, including those on the opposite side of the street and those along other streets.

To mitigate the influence of the sidewalk on the opposite side, an efficient algorithm will be developed based on the C/N0. By applying sidewalk constraints, the number of unknowns in the GNSS problem is reduced from 4 to 2. This transforms the GNSS problem into finding a line that best fits a set of 2D points. Hough Transform is a fundamental algorithm that has been widely used in image processing to find geometric shapes robustly under conditions of multiple outliers [49]. In this study, Hough Transform is applied in the proposed method finding the most consistent measurements under conditions of multiple faults. The contributions of this study include:

(1) For the first time, the use of pedestrian map is proposed to constrain GNSS solutions in urban canyons.

(2) A lightweight algorithm is developed to identify parallel sidewalks on both sides of a street, without the need for complex 3D building models. This algorithm efficiently eliminates unqualified sidewalks, improving the overall positioning solution.

(3) The application of the Hough Transform estimator in GNSS under sidewalk constraints is introduced for the first time. This estimator effectively and robustly searches for consistent measurements, enhancing the GNSS positioning performance.

The remainder of this paper is organized as follows. Section II presents the conventional GNSS FDE algorithms. In Section III, details of the proposed method are formulated and presented. The performance evaluation of the proposed method is presented in Section IV. Finally, the conclusions and future work are presented in Section V.

II. GNSS Fault Detection and Exclusion

The GNSS linear equation can be represented as follows [17, 50]

$$\boldsymbol{\rho} = \boldsymbol{G}\boldsymbol{x} + \boldsymbol{\varepsilon} + \boldsymbol{m} \quad (1)$$

In equation (1), the pseudorange measurement vector, denoted as $\boldsymbol{\rho}$, has a dimension $n \times 1$, where n is the number satellites observed by a receiver. The Jacobian matrix $\boldsymbol{G}$ has a dimension of $n \times 4$, and it contains the unit line-of-sight vectors from satellites to the receiver, followed by a column of ones. The state vector, denoted as $\boldsymbol{x}$, has a dimension 4×1, and it includes 3 coordinates for position and 1 receiver clock bias that is common to all measurements. The measurement error, denoted as $\boldsymbol{\varepsilon}$, has a dimension $n \times 1$. The fault vector, denoted as $\boldsymbol{m}$, has a dimension $n \times 1$ due to multipath or NLOS errors.

The fault vector in Eq. (1) can be defined as:

$$m^s = \begin{cases} 0, & s \in LOS \\ e^s, & s \in NLOS\ or\ multipath \end{cases} \quad (2)$$

where s denotes the index of a satellite ($s = 1,2 \ldots, n$). When the measurement ρ^s does not contain multipath or NLOS error, the corresponding fault m^s is zero. However, if there is a fault, it will introduce a significant bias into the measurement. Typically, NLOS signals result in a positive fault in the measurement, while multipath signals introduce positive and negative error in the measurement.

The weighted least squares estimation of Eq. (1) is given as

$$\hat{\boldsymbol{x}} = (\boldsymbol{G}^T\boldsymbol{W}\boldsymbol{G})^{-1}\boldsymbol{G}^T\boldsymbol{W}\boldsymbol{\rho} \quad (3)$$

where $\boldsymbol{W}$ is a diagonal weighting matrix, with the diagonal elements being the inverse of the variances of measurement errors. The residuals can be calculated by subtracting the predicted measurement from the real measurement

$$\boldsymbol{v} = \boldsymbol{\rho} - \hat{\boldsymbol{\rho}} = (\boldsymbol{I} - \boldsymbol{S})\boldsymbol{\rho}$$
$$= (\boldsymbol{I} - \boldsymbol{S})(\boldsymbol{\varepsilon} + \boldsymbol{m}) \quad (4)$$

where $\boldsymbol{S} = \boldsymbol{G}(\boldsymbol{G}^T\boldsymbol{W}\boldsymbol{G})^{-1}\boldsymbol{G}^T\boldsymbol{W}$.

One of the most widely used test statistics for fault detection and exclusion is the sum of squared residuals t given by

$$t = \boldsymbol{v}^T W \boldsymbol{v} \quad (5)$$

The test statistic t is compared with a threshold to determine if there are any faults in measurements. The residual based FDE method excludes the measurement with the largest normalized residual recursively until t is within the threshold. As shown in Eq. (4), the residuals are in fact a linear combination of different faults, and the large residual can be caused by faults in other measurements. Under the conditions of multiple faults, the largest normalized residual does not necessarily mean that the corresponding measurement is faulty, and the residual based FDE often results in eliminations of fault-free measurements, while retaining faulty measurements.

As opposed to the residual based FDE that uses as many of measurements as possible to get the initial solution, the subset testing method estimates parameters using a minimum number of measurements and tests their consistency with other measurements. This bottom-up method uses a voting scheme to find the most consistent measurements [33]. The application of this method is limited because it is time and computation consuming.

The underlying concept behind the FDE algorithm is that fault-free measurements deliver a more consistent position solution [11, 12]. However, for a pedestrian in urban canyons, the majority of GNSS signals in the cross-street direction are received via NLOS paths caused by buildings on both sides of the street. Under this condition, it is very difficult to detect and exclude faulty measurements based on one or two fault-free measurements in the cross-street direction. Figure 1 illustrates the challenge of FDE due to insufficient redundancy in urban canyons. As shown, the LOS signals and NLOS signals are represented by green and brown lines, respectively. It can be observed that the majority of cross-street satellite signals are blocked by buildings on both sides of the street. The conventional FDE method often finds the consistency using a combination of some faulty and fault-free measurements, significantly degrading the GNSS performance in urban canyons.

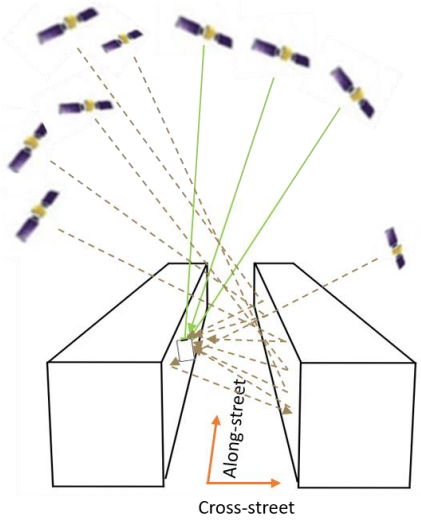

Fig. 1. GNSS positioning in urban canyons

In certain pedestrian or vehicle applications, it is known that the states of the model in Eq. (1) are subject to specific constraints. These constraints can be utilized to increase the redundancy, improving the FDE performance. For instance, height information obtained from a map can be used as a virtual measurement, which proves to be effective in reducing positioning errors. Additionally, in urban canyons, pedestrian positions are subject to sidewalk constraints, presenting an opportunity to enhance urban positioning performance.

III. Pedestrian Map Aided FDE

In urban canyons, pedestrians must walk on sidewalks that are separated from roadway vehicles. Therefore, positions of pedestrians are known to be subject to sidewalk constraints. A pedestrian map provides both walkways in polylines and their height information. The useful constraints derived from the pedestrian map provide additional and virtual references for urban GNSS positioning.

Figure 2 illustrates the benefits of GNSS positioning under sidewalk constraints. As shown, when constraints are not used, the local East, North and Up coordinates must be estimated. The parameter space is reduced to some sidewalks

when the pedestrian map is used to solve for positions.

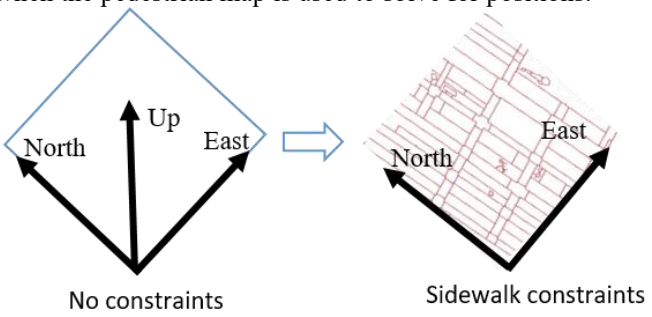

Fig. 2. GNSS positioning under sidewalk constraints

Several candidate sidewalks can be obtained from the pedestrian map centered around an initial position. One approach that could be considered is using the residual based FDE with aid of sidewalk constraints. However, the direct use of the conventional FDE with the sidewalk constraints often leads to determination of positions on wrong sidewalks, resulting in poor accuracy.

In this section, we will use a typical example to show how GNSS accuracy can be improved using the proposed method. The test environment is depicted in Figure 3(a), the true position is near a lamppost situated on the right side of an urban street. The distance between the two parallel sidewalks is approximately 20 meters.

One possible solution is to use the residual based FDE with the constraints of sidewalks. The feasibility of this method is evaluated in this study. Figure 3(b) shows positions from the residual based FDE, with and without sidewalk constraints. If not constrained by sidewalks, GNSS positions are distributed throughout the entire street, including inside buildings. When the sidewalk constraints are applied in the residual based FDE, all positions are determined on sidewalks. However, this method results in frequent position results on other sidewalks, instead of the correct one. This is because the best consistency is often achieved among some fault-free measurements and faulty measurements on the other sidewalks.

Due to the inherent uncertainties in the initial position and the complexity of the pedestrian network, GNSS positions can be determined on other surrounding sidewalks. It is crucial to mitigate the impact of surrounding sidewalks, which can be categorized into two types: (1) sidewalks on the opposite side of the street, as indicated in the black oval in Figure 3 (b); and (2) sidewalks on a different street, being shown in blue oval in Figure 3 (b). To address the former issue, a unique algorithm will be developed to filter out the sidewalk on the opposite side of the street. To tackle the second challenge, a new FDE algorithm based on Hough Transform will be developed.

The purpose of this study is to investigate the use of cross-street constraints to enhance the GNSS FDE performance. Specifically, candidate sidewalks will be first selected and refined. By incorporating this constraint, the redundancy in the cross-street direction can be significantly improved, enabling a reliable detection and elimination of outliers. Consequently, the accuracy of positioning can be greatly enhanced, particularly for sidewalks with narrow widths.

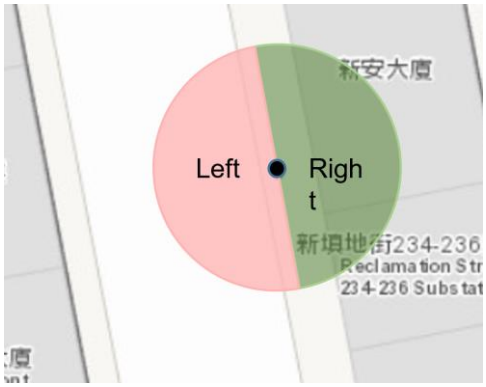

(a)

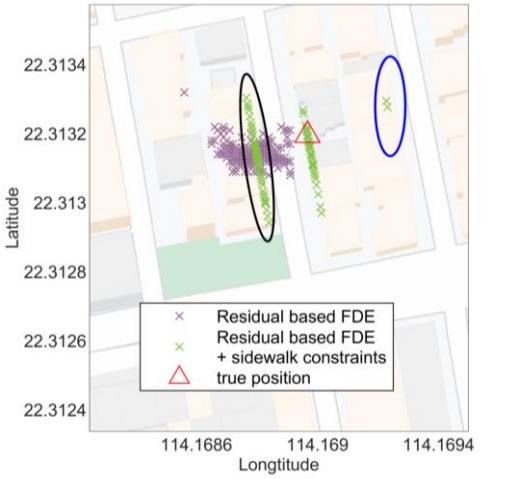

(b)

Fig. 3 An example of position results from residual based FDE without and with sidewalk constraints

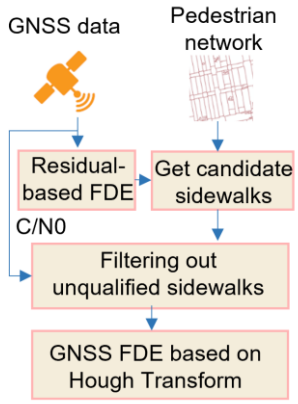

Fig. 4. Flowchart of the FDE method

The flowchart of the proposed method is shown in Figure 4. This method includes three steps. The first step is to generate candidate sidewalks using the initial position on a pedestrian map. It is challenging for current algorithms to distinguish two sides of a street. Therefore, the second step is to filter out the unqualified sidewalks using a new algorithm. Finally, the consistency of GNSS measurements on each candidate sidewalk will be checked using Hough Transform, and positions can be estimated robustly.

A. *Generation of candidate sidewalks on pedestrian map*

The initial GNSS position will be computed using the residual based FDE technique. The search for the solution will be conducted within a circular area centered around the initial position. To ensure that the search region includes the true position, the radius of the circle should be sufficiently large. In this study, considering that the majority of positioning errors from the residual based FDE are within 40 meters, an initial search radius of 40 meters will be employed. If no solution can be obtained within this radius, the search radius will be incrementally increased in an empirical manner to determine the positions.

Suppose that the footpaths derived from the map are represented by line segments l_i, where $i = 1,2 \ldots, N_l$ denotes the index of the line segments and N_l is the number of line segments. Note that each line segment l_i is defined by a pair of beginning and end points, denoted by $(\boldsymbol{s}_i, \boldsymbol{e}_i)$ where $\boldsymbol{s}_i$ and $\boldsymbol{e}_i$ denotes the beginning point and the end point of line segment l_i. Figure 5 illustrates an example of sidewalk generation. As shown, the search region is represented by a circle centred at the initial position with a radius $D = 40$ meters. Four sidewalks are generated from the search region, denoted as l_i: $(\boldsymbol{s}_i, \boldsymbol{e}_i)$ where $i = 1,2,3,4$.

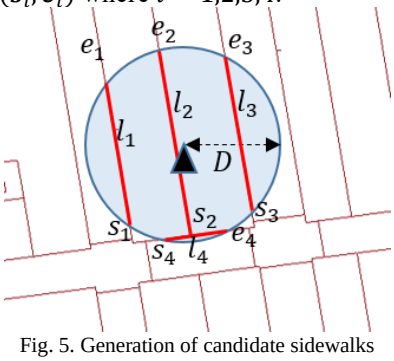

Fig. 5. Generation of candidate sidewalks

The sidewalk constraints reduce the 3-dimentional parameter space to a number of line segments around the pedestrian position. In urban areas, however, there are parallel footpaths on both sides of the street, which are very close to each other. It is challenging for the current algorithm to distinguish between a footpath on one side and another footpath on the opposite side. Rejecting the incorrect sidewalks is particularly important for sidewalk-level positioning, as required by many pedestrian applications.

B. *Filtering out the unqualified sidewalks*

Several candidate sidewalks can be derived from step A, especially when sidewalks are available on both sides of the street. Two sides of the street can potentially be identified using the shadow matching method [35, 45]. However, 3D building models are required. In this study, we will develop a novel algorithm to distinguish two sides of the street based on the fundamental concept of shadow matching method, eliminating the need for 3D building models.

The shadow matching method relies on the variation in sky visibility between different positions, particularly in the cross-street direction. It is achieved by matching the observed C/N0 with the sky visibility. When it is used for identifying the sides of the street, the property of GNSS signals can be explored to two sides of the street. In urban areas, buildings are typically present on both sides of the street in a continuous manner. When a pedestrian walks on a sidewalk adjacent to a building, half of the sky is blocked by this building, and only a part of signals from the other part of sky can be observed. Therefore, the LOS signals observed on two sides of the street are totally different. This property can be used to identify which sidewalk the pedestrian is on.

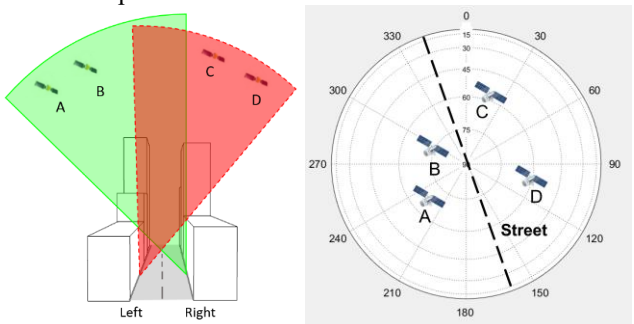

(a) (b)

Fig. 6. Relationship between the LOS signals and the side of the street: (a) different LOS satellites are observed on opposite sides of the street; (b) sky plot for the LOS satellites

The LOS signals observed on two sides of the street are from two parts of the sky, divided by the street direction. That is, LOS signals received on two sides of a street have distinct azimuths that are separated by the direction of the street. This concept is illustrated in Figure 6, which depicts the positions of LOS signals in relation to the street side. In the left panel, the visibility boundaries of the left and right sidewalks are represented by the red and green regions, respectively. The LOS signals from satellites C and D can be observed on the left sidewalk, while the LOS satellites A and B can be observed on the right sidewalk. As shown in the right panel, the azimuth angles of the LOS satellites on two sides of the street are separated by the street direction.

In this study, the observed satellites firstly are categorized into two groups based on the street direction, as illustrated in Figure 6(b). LOS signals are only available in one of the groups, which is dependent on the side of the street where the pedestrian is located in. Therefore, the side of the street can be determined by checking which part has significantly larger number of LOS signals. The C/N0 measurement has been commonly in different methods to distinguish LOS and NLOS signals. This measurement will be used in this algorithm to determine the side of the street. Specifically, we will then check which group has a significantly higher number of satellites with high C/N0 values. For example, if the left group has a substantially larger count of high C/N0 values, the left footpath will be regarded as unsuitable.

The C/N0 can be compared with a predetermined threshold to identify the LOS signals. However, the predetermined threshold method may not reliably identify LOS signals due to potential environmental influences on C/N0. To robustly determine the street side, we will employ a dynamic threshold method that considers the overall distribution of observed C/N0. Initially, the maximum observed C/N0 value will be selected as the threshold. Subsequently, the threshold will be gradually decreased until a group of satellites with C/N0 values surpassing the threshold significantly outnumbers the other group.

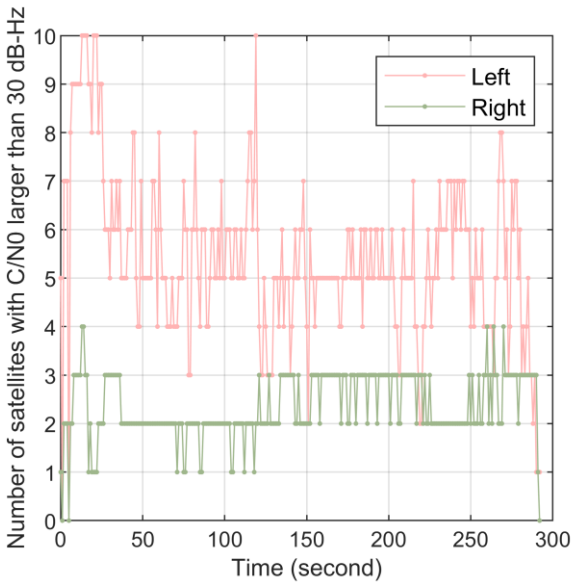

Fig. 7. Number of measurements with C/N0 larger than 30 dB-Hz from two sides of the street

The distribution of C/N0 in the typical example in Figure 3 is evaluated. In Figure 7, the graph displays the number of measurements with a C/N0 value greater than 30 dB-Hz. As anticipated, the majority of satellite signals with high reception power are received from the left side of the sky, or more broadly, the opposite side. This characteristic is used in our FDE algorithm to effectively filter out incorrect candidate sidewalks.

In this study, only the snapshot measurements are used to identify two sides of the street. Due to the large variation of C/N0, the identification performance can be affected by urban environments. Because the LOS signals are similar for the same sidewalk, the identification can be potentially improved using a period of measurements. This part of work will be carried out in future.

In this part, we propose a unique method to determine the side of the street by considering two primary hypotheses: the left and right sides. This method exhibits similarities with shadow matching, although it differs in several aspects. Notably, the proposed method offers the advantage of strong constraints for GNSS FDE, improving the positioning accuracy in both along-track and cross-track directions. In addition, the proposed method utilizes a simple pedestrian network, which is readily accessible and easier to obtain compared to the requirements of shadow matching. Furthermore, the proposed method provides either side of the street instead of multiple possible positions, and the results can be directly used in various map-based applications.

C. Search for pedestrian positions based on Hough Transform

By implementing Step A and Step B, we can select a number of potential sidewalks in the vicinity of the initial position. In this subsequent step, the constraints derived from these sidewalks are used to determine the precise position. Suppose that the number of the candidate sidewalks is reduced from N_l to I after eliminating the unqualified sidewalks in step B. We will solve for positions on each of I candidate sidewalks based on pseudorange measurements. Positions on different sidewalks will be compared, and the position having the maximum consistency will be determined as the final solution.

For each sidewalk, we need to estimate the position on the sidewalk, which is a 1-dimensional positioning problem. We will first transform global coordinate system in Equation (1) to the local coordinate system on the sidewalk, including the along-street, the cross-street and upper components. This transformation is accomplished by applying a rotation matrix R_i calculated from the direction and starting point of the line segment. The cross-street and upper components can be obtained from a sidewalk segment in the pedestrian map. Therefore, the GNSS observation equation on a footpath segment l_i can be expressed as follows:

$$\rho_i^s = g_{a,i}^s \Delta a_i + \Delta t_R + m^s \quad (6)$$

where ρ_i^s is the measurement of satellite s on the footpath l_i; Δa_i denotes the position on the sidewalk; Δt_R represents the receiver clock bias that will be estimated; $g_{a,i}^s$ denotes the parameter for satellite s on the sidewalk i, and it is calculated based on the following equation:

$$g_{a,i}^s = [G \cdot R_i]_{s,1} \quad (7)$$

where $[\cdot]_{s,1}$ denotes an operator for selecting an element at the s-th row and the first column in the matrix.

In Equation (6), $g_{a,i}^s$ and ρ_i^s are two known quantities, while Δa_i and Δt_R are two unknowns that need to be estimated. It can be seen from Equation (6) that the sidewalk constraints introduced in this study reduce the number of unknowns per sidewalk from 4 to 2 for each footpath.

For each satellite s, we know its measurement ρ_i^s and the parameter $g_{a,i}^s$. Different satellites are shown as different points $(g_{a,i}^s, \rho_i^s)$ in the 2D observation space, with X-axis denotes $g_{a,i}^s$ and Y-axis represents ρ_i^s, as illustrated in Figure 8 (a). In this example, there are five fault-free measurements denoted by blue dots, and two faulty measurements indicated by green and black dots. We will then try to find the collinear points, which are essential to estimate two unknowns, namely the position parameter Δa_i and the receiver clock bias Δt_R. They are represented as the slope and the intercept of this collinear line, as shown in Figure 8(a).

The GNSS problem with sidewalk constraints is transformed into finding the best fits of 2D data, which may include multiple outliers, as illustrated in Figure 8(a). This is the classical problem in image processing, which has been addressed using the Hough transform algorithm.

Hough transform is widely used to detect simple geometric shapes in images, which contain a large number of outliers [49]. This estimator is used to robustly identify a line or a circle with high level of noise or outliers in images [51]. GNSS measurements in Equation (6) are also affected by many outliers. In this study, the Hough transform estimator is applied to find the most consistent measurements for each of candidate sidewalks.

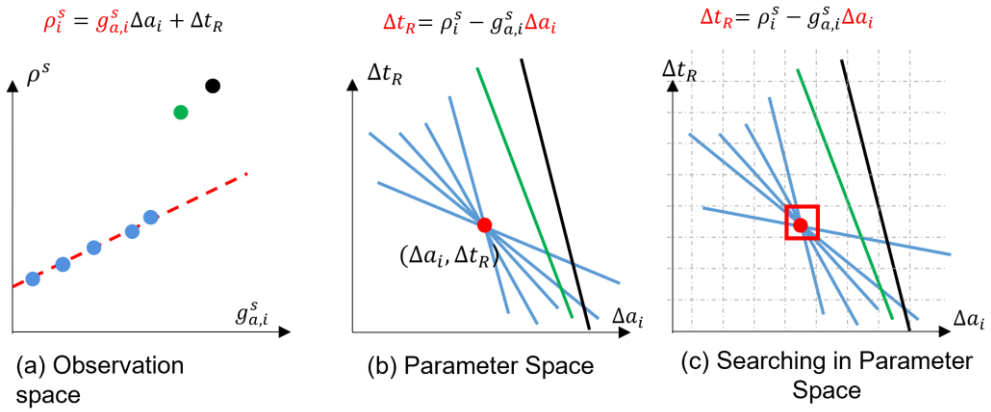

Fig. 8. GNSS positioning on a candidate sidewalk with Hough Transform estimator

The Hough Transform works by transforming the observation space to the parameter space, where the outliers can be detected. To achieve this, Equation (6) is transformed as follows:

$$\Delta t_R = \rho_i^s - g_{a,i}^s \Delta a_i \quad (8)$$

where Δt_R and Δa_i are two unknown parameters we want to estimate. The parameter space of $(\Delta a_i, \Delta t_R)$ represents all possible values these two unknowns, as illustrated in Figure 8(b). By mapping the observation space onto the parameter space, a point in the observation space corresponds to a line in the parameter space, while a line in the observation space corresponds to a point in the parameter space. In the given example, Figure 8(a) shows five collinear points and two outliers. When they are mapped to the parameter space, five intersecting lines and two lines far away are obtained respectively, as shown in Figure 8(b). The intersection of these lines indicates the correct parameters $(\Delta a_i,\ \Delta t_R)$.

To estimate the intercept and slope parameters with the most consistency, the Hough Transform discretizes the parameter space into finite cells and selects the cell with the highest number of lines, as illustrated by the red square in Figure 8(c).

To determine the optimal sidewalk candidate, the Hough Transform is first employed to identify the largest number of consistent measurements on each candidate sidewalk. For each candidate sidewalk l_i, the largest number of consistent measurements $A_i(\Delta t_R, \Delta a_i)$ is found by using the Hough Transform. The sidewalk solution with the largest number of consistent measurements is selected

$$A_{max} = \underset{i}{argmax}\, A_i(\Delta t_R, \Delta a_i) \quad (9)$$

where $A_i(\Delta t_R, \Delta a_i)$ is the number of consistent measurements for a candidate sidewalk l_i. The position that corresponds to this maximum number of consistent measurements is considered the final solution of the algorithm.

The noise level of pseudorange measurements is very large for low-cost GNSS receivers. Therefore, the estimated GNSS positions are finally filtered by employing an extended Kalman filter described in [52] and [53]. In this way, the GNSS positioning accuracy can be further improved.

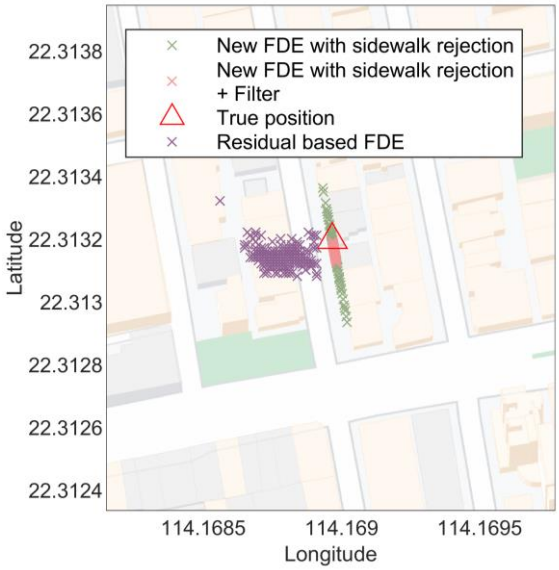

Fig. 9. Positioning results at experimental sites 2: Positioning results of the proposed method

The C/N0 measurements depicted in Figure 7 are further employed to exclude sidewalks that do not meet the required criteria. The positioning results, after eliminating these unqualified sidewalks in advance, are presented in Figure 9. And the positions are then filtered by using the Kalman filter. As illustrated, the proposed algorithm significantly enhances the positioning accuracy for site 2, reducing it from 23.3 m to 5.4 m by effectively filtering out incorrect sidewalks.

IV. Performance Evaluation

In Hong Kong, the precise positions of lampposts have been surveyed by the Lands Department of Hong Kong and made available on the Internet. These lampposts provide valuable information for assessing the performance of the proposed method under different urban environments. In this study, experiments were carried out at 8 lampposts in Mong Kok, a typical urban area in Hong Kong. These lampposts were selected to represent different positioning conditions in terms of building height, street width and direction. Figure 10(a) shows positions of the 8 lampposts.

During the experiments, the pedestrian stood beside each lamppost, and recorded GNSS data for 5 minutes using the

Huawei P40 smartphone. The smartphone supports the GPS and Beidou constellations. Totally, the data collected last about 8*5=40 minutes on 9 December 2020. Each lamppost has a number printed on it, which might be used to find people who might be lost or in trouble, as illustrated in Figure 10(b). By referencing the number on the lamppost, we obtained their precise position from the website of the Lands Department of Hong Kong.

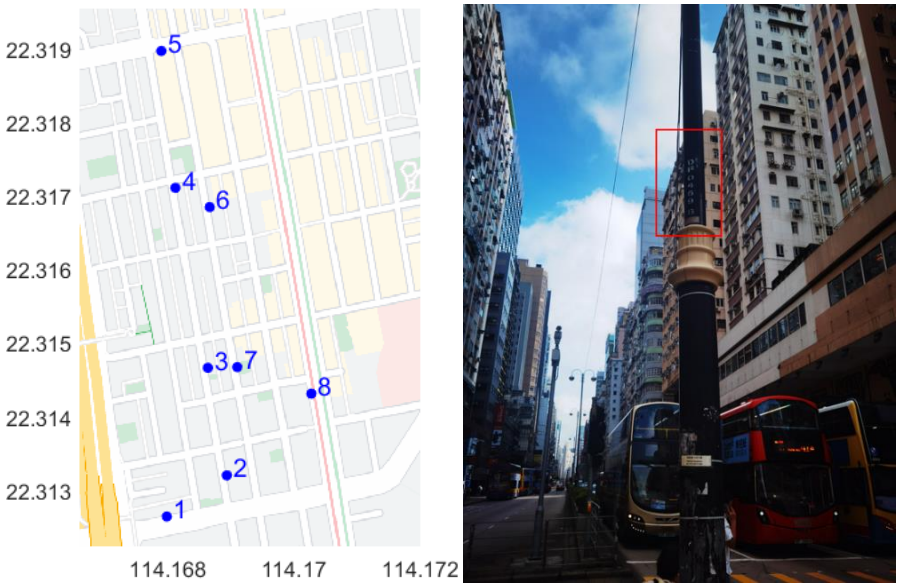

Fig. 10. The performance of the proposed GNSS positioning method is evaluated at eight lampposts with precise location: (a) positions of lampposts (b) the ID printed on the lamppost in urban canyons

The pedestrian positioning system has been developed using the digital pedestrian map provided by the Lands Department of Hong Kong. This map includes 3D pedestrian network, including sidewalks, crosswalks, bridges and underway. Their centerlines are represented by polylines, including latitude, longitude and height information, which are used in the proposed method.

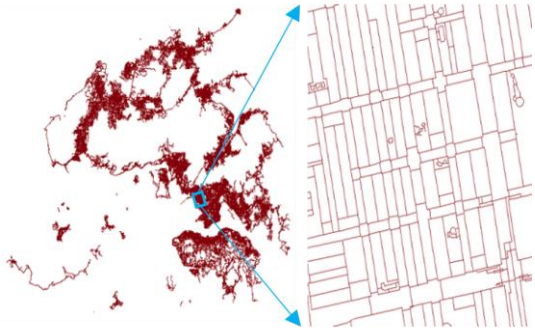

Fig. 11. Overview of the pedestrian network

Figure 11 displays a sample of the pedestrian map. Typically, walkways have a width of 2-3 meters. Hence, if GNSS positions can be accurately determined on the sidewalk, it can lead to a substantial improvement in the performance of urban pedestrian positioning.

Eight sets of GNSS data were collected to evaluate the performance of the proposed method. In each data set, the observed satellites are categorized into two groups: satellites on the same side of the street as the pedestrian and those on the opposite side of the street. The number of satellites with a C/N0 larger than 30 dB-Hz was counted for each group. Figure 12 illustrates the number of qualified satellites received from both sides for the eight experimental sites. On average, the number of satellites received from the opposite side was 6.8, while the number of satellites received from the same side was 2.4. The results clearly indicate that a greater number of qualified satellites are received from the opposite side compared to the same side. Consequently, the proposed algorithm successfully rejects incorrect sidewalks with a success rate of 92%.

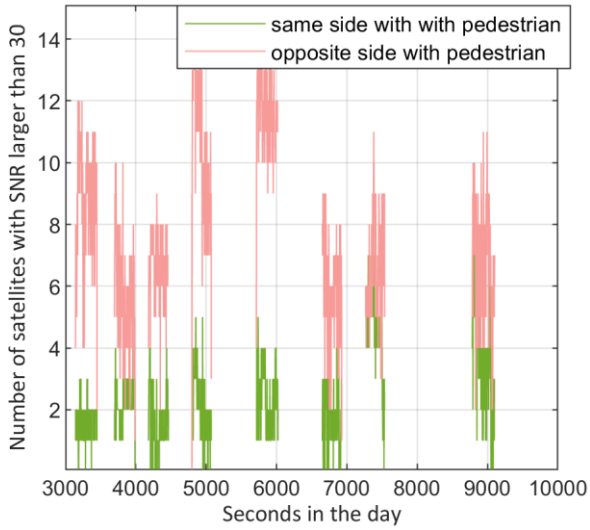

Fig. 12. Number of qualified satellites received from the same side of the street as the pedestrian and the opposite side of the street

Figure 13 shows positioning results from the residual based FDE and the proposed method for the 8 test points. As shown, the residual based FDE results in a much larger cross-street position error, compared with the along-street position error.

With the proposed method, the cross-street direction positioning error is significantly reduced with the use of the sidewalk constraints.

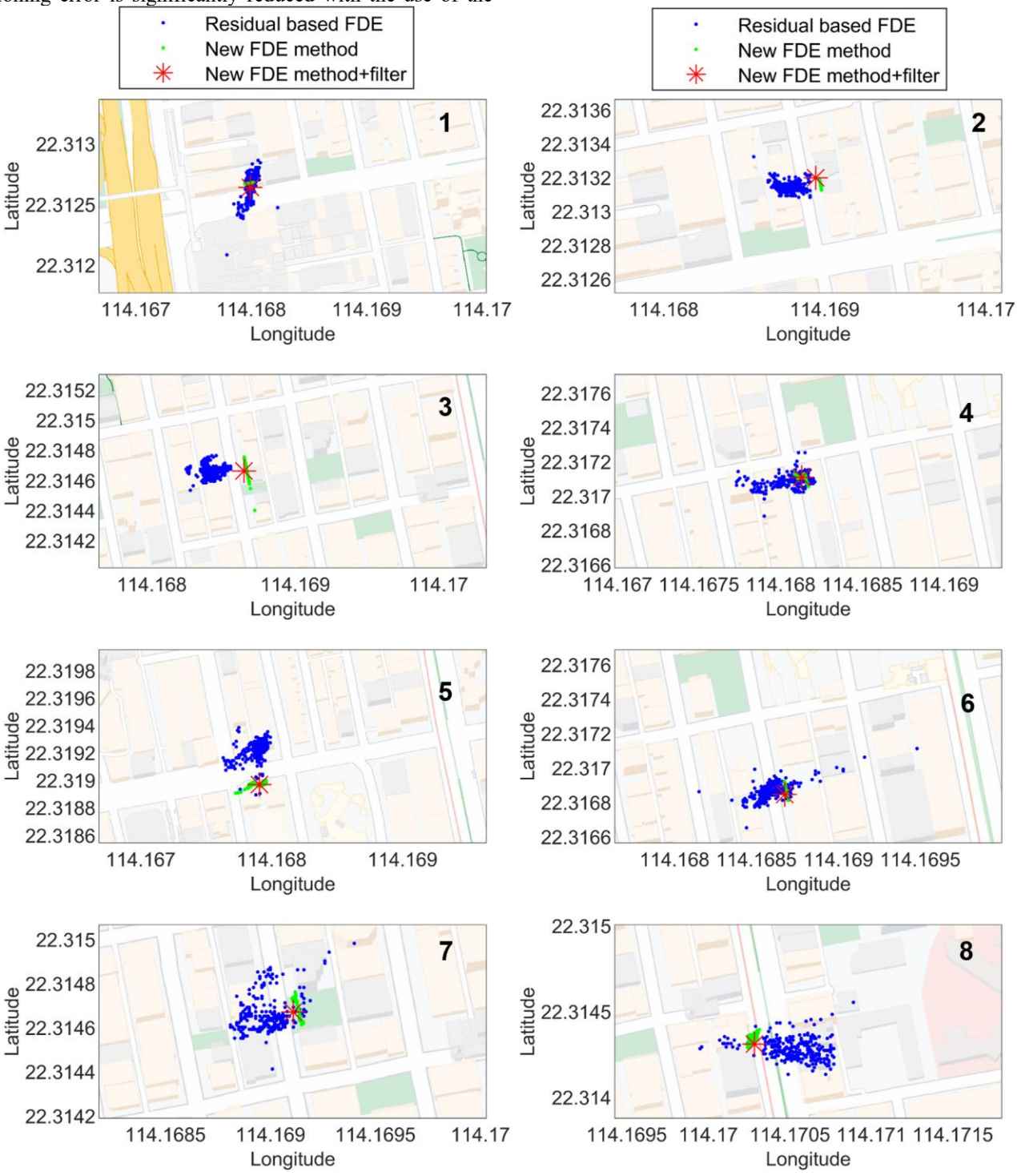

Fig. 13. Positions delivered by the residual based FDE and the novel FDE method for eight points

Positioning errors were calculated by comparing the positioning results with the true position, and RMS errors for eight experimental sites were shown in Figure 14. The residual based FDE results in a position accuracy of 22 m, and the proposed method delivers a positioning accuracy of 4.9 m. More importantly, all the GNSS positions are solved under constraints of sidewalks, and results show that the sidewalk-level GNSS positioning in urban areas is achievable through the proposed method.

A dynamic test was performed by a pedestrian walking around a block in Mong Kok, Hong Kong, lasting approximately 7 minutes. The test route includes four sidewalks. The smartphone P40 was used in this test to collect GNSS data.

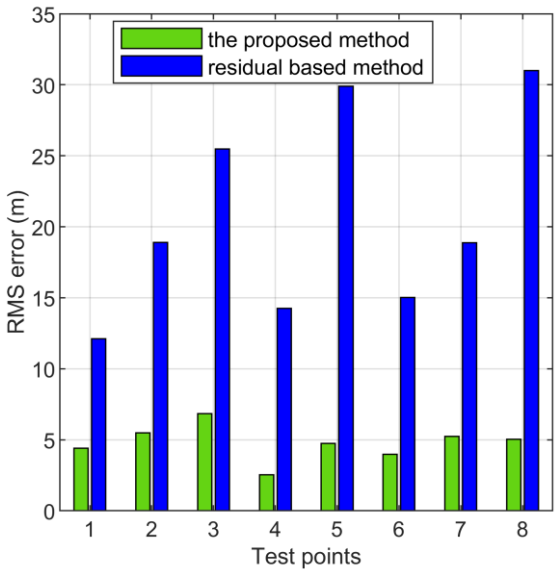

Fig. 14. Comparison of RMS errors between the residual based FDE and the new FDE method

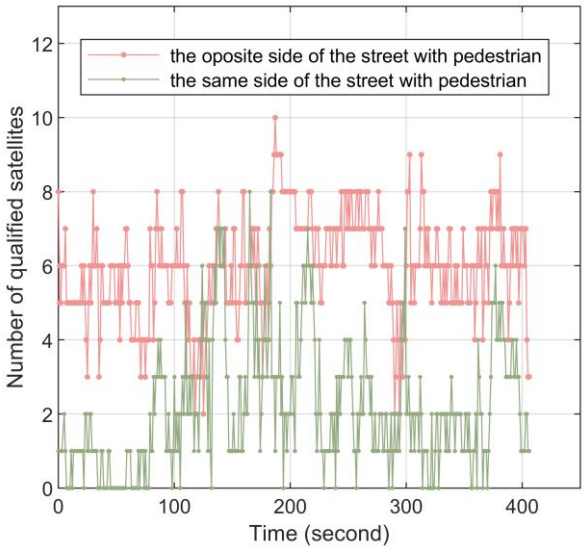

Fig. 15. Number of qualified satellites received from the same side of the street as the pedestrian and the opposite side of the street

Figure 15 shows the number of the qualified satellites received from the same side of the street as the pedestrian and the opposite side of the street. Under normal conditions, the number of the qualified satellites observed from the opposite side is significantly larger than that observed from the same side as the pedestrian. There are some cases, where two the similar number of the qualified satellites are observed from two sides. These happen when the pedestrian is on the crossway or at the corner of the street.

Figure 16 shows the positioning solution from the conventional residual method and the proposed method. As shown, positions obtained using the proposed method are depicted by the green line, while those obtained using the conventional method are represented by the blue dots. Due to the absence of reference points, a detailed accuracy analysis was conducted. However, when comparing the results with Google Maps, it is evident that the proposed method greatly improves positioning accuracy, achieving the sidewalk level positioning.

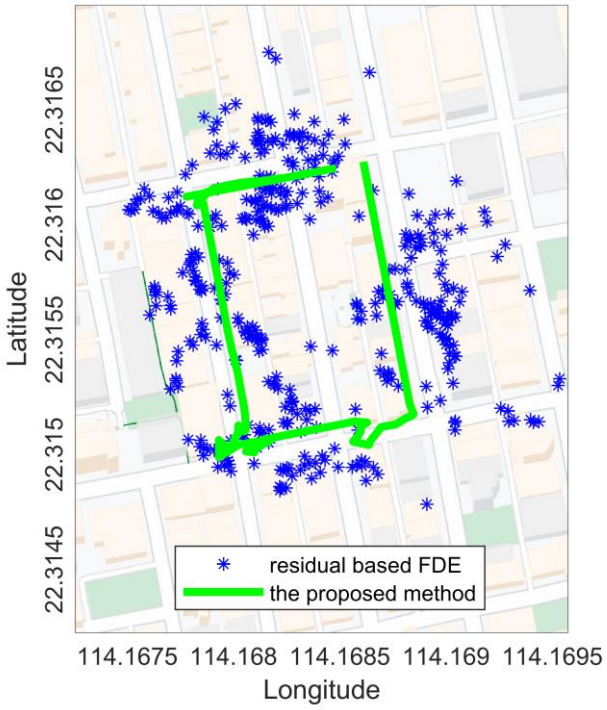

Fig. 16. Dynamic test results in Mong Kok, Hong Kong

It can also be concluded that the wrong sidewalk can be determined at the crossway or at the corner using the proposed method. This challenge can be further investigated by considering sequential dynamic or by using pedestrian dead reckoning system, which will be conducted in future work.

V. Conclusions and Future Work

This paper presents the first urban GNSS positioning method for pedestrians using pedestrian network. A unique algorithm is proposed to distinguish two sides of the street. This algorithm uses the fundamental concept of shadow matching algorithm, but it does not require 3D building models. The new algorithm is built on the fact that LOS signals received on two sides of a street have distinct azimuths that are separated by the street direction. To further enhance the FDE performance under sidewalk constraints, GNSS positions are solved using the Hough Transform estimator. The performance of the novel method is evaluated using GNSS data from both static and dynamic tests.

We analysed the C/N0 observations collected at the eight lampposts. Results showed that 92% of sidewalks can be distinguished from the opposite sidewalk along the same street. The proposed FDE algorithm improves the positioning accuracy from 22 m to 4.9 m, a 77% improvement over residual based FDE search algorithm. We also conducted a dynamic test around a block in the urban canyon. Results show that the positioning performance is greatly improved.

The proposed method improves the performance of urban GNSS performance with the aid of a pedestrian map. The advantages of this method include: 1) urban GNSS positioning

accuracy is improved with sidewalk constraints; 2) multiple faults can be detected and excluded efficiently by searching in parameter space; 3) this method achieves the sidewalk-level accuracy, benefiting lots of pedestrian applications. It can be scaled to other cities that have a pedestrian map available. This map represents each sidewalk by specifying its starting position and ending position, which are used to constrain pedestrian positions effectively.

The method proposed in this study can be used to augment GNSS in urban areas when the pedestrian is walking on sidewalks adjacent to buildings. In urban areas, pedestrians can also walk in open spaces, on crossways, underground tunnels. The proposed method does not work properly under these conditions. In the next step, the integration of GNSS, pedestrian network and inertial sensors will be conducted in future to achieve seamless pedestrian navigation in urban canyons.

The proposed method not only improves urban GNSS performance but also opens up opportunities for new applications, such as jaywalking monitoring and last-mile delivery. By addressing the issue of jaywalking, which has been identified as a significant contributor to traffic collisions and pedestrian fatalities, the proposed method has the potential to contribute to reducing the alarming statistic of approximately 1.35 million deaths annually, with pedestrians and cyclists accounting for half of the victims [54]. With its ability to accurately distinguish between sidewalks and provide sidewalk-level accuracy, the proposed method can be effectively utilized for jaywalking monitoring, enhancing pedestrian safety, and contributing to the overall improvement of road user protection.

REFERENCES

[1] F. Zangenehnejad and Y. Gao, "GNSS smartphones positioning: Advances, challenges, opportunities, and future perspectives," *Satellite navigation*, vol. 2, pp. 1-23, 2021.

[2] A. Giremus, J.-Y. Tourneret, and V. Calmettes, "A particle filtering approach for joint detection/estimation of multipath effects on GPS measurements," *IEEE Transactions on Signal Processing*, vol. 55, no. 4, pp. 1275-1285, 2007.

[3] H. Kim and J. Ben-Othman, "Eco-friendly low resource security surveillance framework toward green AI digital twin," *IEEE Communications Letters*, vol. 27, no. 1, pp. 377-380, 2022.

[4] D. Weng, S. Ji, Y. Lu, W. Chen, and Z. Li, "Improving DGNSS performance through the use of network RTK corrections," *Remote Sensing*, vol. 13, no. 9, p. 1621, 2021.

[5] D. Weng, S. Ji, W. Chen, Z. Li, Y. Xu, and L. Ye, "Assessing and mitigating the effects of the ionospheric variability on DGPS," *GPS solutions*, vol. 19, pp. 107-116, 2015.

[6] W. W. Wen, G. Zhang, and L.-T. Hsu, "GNSS NLOS exclusion based on dynamic object detection using LiDAR point cloud," *IEEE transactions on intelligent transportation systems*, vol. 22, no. 2, pp. 853-862, 2019.

[7] W. W. Wen and L.-T. Hsu, "3D LiDAR aided GNSS NLOS mitigation in urban canyons," *IEEE Transactions on Intelligent Transportation Systems*, vol. 23, no. 10, pp. 18224-18236, 2022.

[8] D. Weng, Z. Hou, Y. Meng, M. Cai, and Y. Chan, "Characterization and mitigation of urban GNSS multipath effects on smartphones," *Measurement*, vol. 223, p. 113766, 2023.

[9] B. Xu, Q. Jia, and L.-T. Hsu, "Vector tracking loop-based GNSS NLOS detection and correction: Algorithm design and performance analysis," *IEEE transactions on instrumentation and measurement*, vol. 69, no. 7, pp. 4604-4619, 2019.

[10] L. Wang, P. D. Groves, and M. K. Ziebart, "Smartphone shadow matching for better cross-street GNSS positioning in urban environments," *The Journal of Navigation*, vol. 68, no. 3, pp. 411-433, 2015.

[11] L.-T. Hsu, H. Tokura, N. Kubo, Y. Gu, and S. Kamijo, "Multiple faulty GNSS measurement exclusion based on consistency check in urban canyons," *IEEE Sensors Journal*, vol. 17, no. 6, pp. 1909-1917, 2017.

[12] P. D. Groves and Z. Jiang, "Height aiding, C/N0 weighting and consistency checking for GNSS NLOS and multipath mitigation in urban areas," *The Journal of Navigation*, vol. 66, no. 5, pp. 653-669, 2013.

[13] Y. Choi and H. Kim, "Convex Hull Obstacle-Aware Pedestrian Tracking and Target Detection in Theme Park Applications," *Drones*, vol. 7, no. 4, p. 279, 2023.

[14] R. G. Brown, "A baseline GPS RAIM scheme and a note on the equivalence of three RAIM methods," *Navigation*, vol. 39, no. 3, pp. 301-316, 1992.

[15] Z. Z. M. Kassas, M. Maaref, J. J. Morales, J. J. Khalife, and K. Shamei, "Robust vehicular localization and map matching in urban environments through IMU, GNSS, and cellular signals," *IEEE Intelligent Transportation Systems Magazine*, vol. 12, no. 3, pp. 36-52, 2020.

[16] W. Wen and L.-T. Hsu, "Towards robust GNSS positioning and real-time kinematic using factor graph optimization," in *2021 IEEE International Conference on Robotics and Automation (ICRA)*, 2021: IEEE, pp. 5884-5890.

[17] J. Lesouple, T. Robert, M. Sahmoudi, J.-Y. Tourneret, and W. Vigneau, "Multipath mitigation for GNSS positioning in an urban environment using sparse estimation," *IEEE Transactions on Intelligent Transportation Systems*, vol. 20, no. 4, pp. 1316-1328, 2018.

[18] W. Y. Ochieng, K. Sauer, D. Walsh, G. Brodin, S. Griffin, and M. Denney, "GPS integrity and potential impact on aviation safety," *The journal of navigation*, vol. 56, no. 1, pp. 51-65, 2003.

[19] N. Zhu, J. Marais, D. Bétaille, and M. Berbineau, "GNSS position integrity in urban environments: A review of literature," *IEEE Transactions on Intelligent Transportation Systems*, vol. 19, no. 9, pp. 2762-2778, 2018.

[20] J. E. Angus, "RAIM with multiple faults," *Navigation*, vol. 53, no. 4, pp. 249-257, 2006.

[21] M. Caamano, O. G. Crespillo, D. Gerbeth, and A. Grosch, "Detection of GNSS multipath with time-differenced code-minus-carrier for land-based applications," in *2020 European Navigation Conference (ENC)*, 2020: IEEE, pp. 1-12.

[22] W. Li, X. Zhu, Z. Chen, Z. Dai, J. Li, and C. Ran, "Code multipath error extraction based on the wavelet and empirical mode decomposition for Android smart devices," *GPS Solutions*, vol. 25, no. 3, p. 91, 2021.

[23] H. Wen, S. Pan, W. Gao, Q. Zhao, and Y. Wang, "Real-time single-frequency GPS/BDS code multipath mitigation method based on C/N0 normalization," *Measurement*, vol. 164, p. 108075, 2020.

[24] G. Zhang, P. Xu, H. Xu, and L.-T. Hsu, "Prediction on the urban GNSS measurement uncertainty based on deep learning networks with long short-term memory," *IEEE Sensors Journal*, vol. 21, no. 18, pp. 20563-20577, 2021.

[25] Q. Liu *et al.*, "NLOS signal detection and correction for smartphone using convolutional neural network and variational mode decomposition in urban environment," *GPS Solutions*, vol. 27, no. 1, p. 31, 2023.

[26] Z. Jiang, P. D. Groves, W. Y. Ochieng, S. Feng, C. D. Milner, and P. G. Mattos, "Multi-constellation GNSS multipath mitigation using consistency checking," in *Proceedings of the 24th International Technical Meeting of The Satellite Division of the Institute of Navigation (ION GNSS 2011)*, 2011, pp. 3889-3902.

[27] M. Joerger and B. Pervan, "Fault detection and exclusion using solution separation and chi-squared ARAIM," *IEEE Transactions on Aerospace and electronic systems*, vol. 52, no. 2, pp. 726-742, 2016.

[28] M. Joerger, F. C. Chan, and B. Pervan, "Solution separation versus residual-based RAIM," *NAVIGATION: Journal of the Institute of Navigation*, vol. 61, no. 4, pp. 273-291, 2014.

[29] R. G. Brown and P. W. McBurney, "Self-Contained GPS Integrity Check Using Maximum Solution Separation," *Navigation*, vol. 35, no. 1, pp. 41-53, 1988.

[30] J. Blanch, T. Walter, and P. Enge, "RAIM with optimal integrity and continuity allocations under multiple failures," *IEEE Transactions on Aerospace and Electronic Systems*, vol. 46, no. 3, pp. 1235-1247, 2010.

[31] R. Sun, J. Wang, Q. Cheng, Y. Mao, and W. Y. Ochieng, "A new IMU-aided multiple GNSS fault detection and exclusion algorithm for integrated navigation in urban environments," *GPS Solutions*, vol. 25, pp. 1-17, 2021.

[32] K. Zhang and P. Papadimitratos, "Fast Multiple Fault Detection and Exclusion (FM-FDE) Algorithm for Standalone GNSS Receivers," *IEEE Open Journal of the Communications Society*, vol. 2, pp. 217-234, 2021.

[33] G. Castaldo, A. Angrisano, S. Gaglione, and S. Troisi, "P-RANSAC: An Integrity Monitoring Approach for GNSS Signal Degraded Scenario," *International Journal of Navigation & Observation*, 2014.

[34] P. D. Groves, Z. Jiang, L. Wang, and M. K. Ziebart, "Intelligent urban positioning using multi-constellation GNSS with 3D mapping and NLOS signal detection," in *Proceedings of the 25th International Technical Meeting of The Satellite Division of the Institute of Navigation (ION GNSS 2012)*, 2012, pp. 458-472.

[35] L. Wang, P. D. Groves, and M. K. Ziebart, "GNSS shadow matching: Improving urban positioning accuracy using a 3D city model with optimized visibility scoring scheme," *NAVIGATION: Journal of the Institute of Navigation*, vol. 60, no. 3, pp. 195-207, 2013.

[36] M. M. Atia and S. L. Waslander, "Map-aided adaptive GNSS/IMU sensor fusion scheme for robust urban navigation," *Measurement*, vol. 131, pp. 615-627, 2019.

[37] J. Wang, W. Chen, D. Weng, W. Ding, and Y. Li, "Barometer assisted smartphone localization for vehicle navigation in multilayer road networks," *Measurement*, vol. 211, p. 112661, 2023.

[38] C. Zhuang, H. Zhao, S. Hu, X. Meng, and W. Feng, "A Novel GNSS Fault Detection and Exclusion Method for Cooperative Positioning System," *IEEE Transactions on Vehicular Technology*, 2022.

[39] N. Alam and A. G. Dempster, "Cooperative positioning for vehicular networks: Facts and future," *IEEE transactions on intelligent transportation systems*, vol. 14, no. 4, pp. 1708-1717, 2013.

[40] L.-T. Hsu, Y. Gu, Y. Huang, and S. Kamijo, "Urban pedestrian navigation using smartphone-based dead reckoning and 3-D map-aided GNSS," *IEEE Sensors Journal*, vol. 16, no. 5, pp. 1281-1293, 2015.

[41] H.-F. Ng, G. Zhang, and L.-T. Hsu, "Robust GNSS shadow matching for smartphones in urban canyons," *IEEE Sensors Journal*, vol. 21, no. 16, pp. 18307-18317, 2021.

[42] M. Adjrad and P. D. Groves, "Enhancing least squares GNSS positioning with 3D mapping without accurate prior knowledge," *Navigation: Journal of The Institute of Navigation*, vol. 64, no. 1, pp. 75-91, 2017.

[43] S. Miura, L.-T. Hsu, F. Chen, and S. Kamijo, "GPS error correction with pseudorange evaluation using three-dimensional maps," *IEEE Transactions on Intelligent Transportation Systems*, vol. 16, no. 6, pp. 3104-3115, 2015.

[44] D. Betaille, F. Peyret, M. Ortiz, S. Miquel, and F. Godan, "Improving accuracy and integrity with a probabilistic Urban Trench modeling," *Navigation: Journal of The Institute of Navigation*, vol. 63, no. 3, pp. 283-294, 2016.

[45] S. Bhamidipati, S. Kousik, and G. Gao, "Set-Valued Shadow Matching Using Zonotopes for 3D-Map-Aided GNSS Localization," *NAVIGATION: Journal of the Institute of Navigation*, vol. 69, no. 4, 2022.

[46] L. C. Bento, P. Bonnifait, and U. J. Nunes, "Set-membership position estimation with GNSS pseudorange error mitigation using lane-boundary measurements," *IEEE Transactions on Intelligent Transportation Systems*, vol. 20, no. 1, pp. 185-194, 2018.

[47] R. Toledo-Moreo, D. Bétaille, F. Peyret, and J. Laneurit, "Fusing GNSS, dead-reckoning, and enhanced maps for road vehicle lane-level navigation," *IEEE Journal of Selected Topics in Signal Processing*, vol. 3, no. 5, pp. 798-809, 2009.

[48] J. Gabela, A. Kealy, M. Hedley, and B. Moran, "Case study of Bayesian RAIM algorithm integrated with Spatial Feature Constraint and Fault Detection and Exclusion algorithms for multi-sensor positioning," *Navigation*, vol. 68, no. 2, pp. 333-351, 2021.

[49] J. Illingworth and J. Kittler, "A survey of the Hough transform," *Computer vision, graphics, and image processing*, vol. 44, no. 1, pp. 87-116, 1988.

[50] D. Weng, W. Chen, Y. Lu, S. Ji, H. Luo, and M. Cai, "Global DGNSS service for mobile positioning through public corrections," *Advances in Space Research*, 2023.

[51] P. Mukhopadhyay and B. B. Chaudhuri, "A survey of Hough Transform," *Pattern Recognition*, vol. 48, no. 3, pp. 993-1010, 2015.

[52] H. Luo *et al.*, "Integration of GNSS and BLE technology with inertial sensors for real-time positioning in urban environments," *IEEE Access*, vol. 9, pp. 15744-15763, 2021.

[53] J. Ye, Y. Li, H. Luo, J. Wang, W. Chen, and Q. Zhang, "Hybrid urban canyon pedestrian navigation scheme combined PDR, GNSS and beacon based on smartphone," *Remote Sensing*, vol. 11, no. 18, p. 2174, 2019.

[54] S. K. Ahmed *et al.*, "Road traffic accidental injuries and deaths: A neglected global health issue," *Health science reports*, vol. 6, no. 5, p. e1240, 2023.

Duojie Weng received the B.S. and M.S. degrees in electrical engineering from Hohai University, Nanjing, China in 2007 and 2010, and the Ph.D. degree from The Hong Kong Polytechnic University, Hong Kong, in 2016. He is currently a Research Assistant Professor with the Department of Land Surveying and Geo-Informatics, The Hong Kong Polytechnic University, Hong Kong. His research interests include urban positioning, high-precision GNSS, sensor integration.

Miaomiao Cai received the Ph.D. degree from the East China Normal University. She is currently a Postdoctoral research Fellow with the Hong Kong Polytechnic University. His research interests include GNSS real-time high accuracy positioning and multi-sensor fusion techniques.

Wu Chen received his Ph.D. degree from Newcastle University, Newcastle upon Tyne, UK, in 1992.

He is currently a Professor with the Department of Land Surveying and Geo-Informatics, The Hong Kong Polytechnic University, Hong Kong. His current research interests include the GNSS positioning quality evaluation, system integrity, various GNSS applications, seamless positioning, and SLAM.

Jingxian Wang received his B.S. degrees and M.S. degrees from Nanjing University of Aeronautics and Astronautics, Nanjing, China, in 2015 and 2018. He is currently pursuing the Ph.D. degree with the Department of Land Surveying and Geo-Informatics, The Hong Kong Polytechnic University, Hong Kong.

His current research interests include multi-sensors fusion, indoor position, pedestrian, and vehicle navigation.

Shengyue Ji is an Associate Profession with China University of Petroleum (East China), Qingdao, China. His interests include GNSS Applications on Transportation, Kinematic GPS, GNSS Performance Evaluation, Regional GPS Network, algorithm development, Vehicle and Personal Navigation Systems, and Wireless Sensor Network.